Enthalpy−Entropy and Cavity Decomposition of Alkane Hydration Free Energies: Numerical Results and Implications for Theories of Hydrophobic Solvation

E. Gallicchio, M. M. Kubo, and R. M. Levy*

Department of Chemistry, Rutgers University, Piscataway, New Jersey 08854

Received: February 17, 2000; In Final Form: April 17, 2000

This study reports the first complete description of the solution thermodynamics of a series of linear, branched, and cyclic alkanes in water by computer simulations, including the enthalpy and entropy changes in addition to the solvation free energies. We have also obtained a complete thermodynamic description of the solvation of the associated alkane cavities. Our results lead to the following key observations: (i) The theoretical prediction that hydration entropy and solvent reorganization are weakly coupled to solute−solvent dispersion interactions is confirmed by computer simulations. (ii) The weak correlation between solute−solvent dispersion interaction energies with solute surface area explains the large relative solubilities of cyclic alkanes and the large difference between the free energy/surface area relations observed for gas to water transfer processes compared to processes involving conformational rearrangements. (iii) The work of cavity formation in water is determined in about equal measure by unfavorable entropic and solvent reorganization energy effects. The findings obtained in this work have important implications for theories of hydrophobicity and suggest an approach to parametrize the free energies of apolar hydration and association.

1. Introduction

The study of hydrophobic hydration and hydrophobic interactions is of importance in many scientific fields.[1] In particular, water-induced nonpolar interactions[2] play a very important role in biological systems from micelle and cell membranes formation[3] to protein folding[4−6] and ligand binding.[7−9]

Hydrophobic hydration constitutes one of the two basic prototypes for studying the forces that determine the structure of solutions and the thermodynamics of solvation, yet molecular theories of hydrophobicity remain a matter of debate in the copious literature still produced on the subject.[10] According to the iceberg model of Frank and Evans,[11] the large entropy loss and the large enthalpy gain upon dissolution of an apolar molecule in water is due to the formation of low-energy rigid water structures around the solute. This view has been criticized in other studies[12] that find that hydrophobic effects can be rationalized simply on the basis of the small size of water molecules. Explicit solvent computational studies[13] of apolar systems in water have provided important thermodynamic and structural information concerning the origins of hydrophobicity.[14−25] Although some studies support the traditional view that water tends to form low-energy cage structures around apolar solutes, they also show that such water cage structures are not rigid. Computational studies also show that the association of apolar molecules in water is less predictable than previously thought as it is not only entropy driven but specific solvent effects exist that may favor solvent-separated solute pairs.

The majority of the existing hydrophobicity models have emerged from computational studies of simple nonpolar monatomic solutes; it is not straightforward to use them to predict the solvation thermodynamics of complex molecular species, like proteins, containing larger apolar regions. Whereas accurate models of electrostatic interactions have emerged,[13,26−29] there is evidence that the current empirical models of nonpolar hydration as applied to even simple hydrocarbons require further improvements. In particular, parametrizations based on the solute solvent accessible surface area[30,31] are found to be unable to accurately fit the hydration free energies of different conformations of linear, branched, and cyclic hydrocarbons with a single proportionality constant.[32−34]

For these reasons we have extended previous studies of the thermodynamics of hydrophobicity by studying more complex molecular species and extracting more detailed thermodynamic information beyond the hydration free energy. In this work we investigate the free energies, enthalpies, and entropies of hydration of the alkanes from 1 to 5 carbon atoms, cyclopentane, cyclohexane, and several conformations of hexane by explicit solvent free energy perturbation (FEP) calculations. The hydration process is further divided into the work of cavity formation followed by insertion of the solute in the cavity. This study provides a picture of the thermodynamics of alkane hydration that is not obtainable by experimental means alone and has not been obtained before by computational means.

Alkane aqueous solutions have been extensively studied using explicit solvent calculations.[35−38] The present study extends previous studies of alkane hydration already reported[39−41] in several ways: (i) A larger set of alkanes including branched and cyclic alkanes is examined. (ii) The hydration process is split into the work of cavity formation and work of formation of solute−solvent dispersion interactions. (iii) In addition to the free energies, enthalpy and entropy changes are evaluated.

We have investigated a larger set of alkanes to explore the connection between structures and thermodynamic properties. Whereas the solvation properties of normal alkanes necessarily scale linearly with the size of the chain, branched and, more clearly, cyclic alkanes, present anomalous hydration properties that must be understood in order to develop an accurate empirical model for nonpolar hydration applicable to a larger

* Corresponding author.

10.1021/jp0006274 CCC: $19.00
Published on Web 06/01/2000

variety of molecular moieties. This task is difficult because the hydration free energies of the alkanes are relatively small and present small variations that are difficult to rationalize. The larger solubility of cyclic alkanes with respect to normal alkanes is a phenomenon still not clearly understood. A meaningful decomposition of the hydration free energies should show patterns that can help in this understanding. In this work we decompose the hydration free energies into cavity/dispersion terms and entropic/enthalpic terms.

The solvation properties of hydrophobic species are determined by their excluded solvent volume and their attractive van der Waals interactions with the solvent. The two effects can be studied independently[42] by subdividing the total solvation process into two steps. In the first step a suitable cavity is created in the solvent; in the second step the attractive interactions between the solute and the solvent are established.[12,43,44] This decomposition offers additional perspectives on the origin of hydrophobicity and allows us to connect with solution theories that treat hydrophobic solutes as collections of hard spheres.[42,45,46] The repulsive solute cavity is essentially a void in the solvent matrix and represents the most basic form of hydrophobic species. The connection between cavity shape and cavity hydration free energy should therefore be applicable to a large range of solutes and should represent the first step in the study of hydrophobicity. On the other hand, the free energies associated with the solute−solvent attractive terms are expected to depend on more specific molecular features such as type of constituent atoms and their number and location.

The entropy/enthalpy decomposition[13,47] of the free energies can lead to additional insights. First, because hydration entropies and enthalpies are experimentally measurable quantities, calculated hydration entropies and enthalpies can be compared to the experiments to assess the quality of the model used in the calculation. Second, because the entropies and enthalpies are thermodynamic state functions, the entropy/enthalpy decomposition does not depend on the particular thermodynamic path taken to solvate the solute (in the cavity/attraction decomposition, instead, cavity formation must precede the establishment of the dispersion interactions). Moreover, because hydrophobic hydration is characterized by particular signatures found mainly in the enthalpies and entropies of solvation,[48] invariably the analysis of the free energy changes obtained involves the analysis of the relative importance of the corresponding enthalpy and entropy changes.

The solvent reorganization energy is a key quantity that we have obtained to determine the enthalpies and entropies of hydration. Solvent reorganization in hydrophobic hydration is poorly understood given the complexity of the phenomenon, the multiple possible interpretations of the experimental data, and the stringent computational resources required in order to study it by computer simulations. A number of computational and theoretical studies have focused on the role of solvent reorganization around a hydrophobic solute.[13] In most of these studies the solute is just a sphere or a monatomic solute,[17,18,20,46,49,50] a system that is probably too simplistic to describe the large variability of shapes of nonpolar molecular moieties found in biological systems. Several approximate methods have been proposed[50−54] to study solvent reorganization upon hydration of complex nonpolar solutes. In this paper the solvent reorganization is calculated directly from the computer simulations and the accuracy of the method is evaluated. The estimates of the solvent reorganization energy obtained are used to discuss the ability of water to adapt to the presence of the apolar solute by minimizing the loss of water−water interactions and its effect on the solubilities of the alkanes.

The enthalpy/entropy and cavity/dispersion decompositions are not independent. It has been postulated[42] that whereas cavity creation in water is accompanied by entropy loss and solvent reorganization, the solute−solvent attractive interactions in first approximation do not change the solvent structure and therefore they affect the hydration enthalpy but not the hydration entropy and the solvent reorganization energy. In this work, we confirm this conjecture by explicit numerical calculations and we give quantitative estimates of the entropy loss and of the solvent reorganization energy upon cavity formation. This analysis also suggests a physically motivated route to the parametrization of the thermodynamics of hydrophobic hydration. We show that the cavity hydration free energies, although difficult to calculate explicitly, are, nevertheless, well correlated with the solvent accessible area of the solute. In contrast, the solute−solvent dispersion interaction energies of the small hydrocarbons studied here are almost independent of surface area but do depend strongly on atomic composition.

2. Methods

2.1. Free Energy. The solvation free energy differences between two solutes X and Y are computed by the free energy perturbation (FEP)[55−58] method. In our implementation, the geometry parameters (bond lengths, bond angles, and dihedral angles) and the potential function parameters (charges and Lennard-Jones parameters) depend on the charging variable λ in such a way that by going from $\lambda = 0$ to $\lambda = 1$ the parameters corresponding to the solute X are transformed into the parameters corresponding to the solute Y. This is accomplished in several steps. In the ith step λ assumes the value λ_i and the system parameters are set accordingly. The Gibbs free-energy change for the ith window obtained by varying λ from λ_i to λ_{i+1} is expressed as

$$\Delta G(i+1, i) = -kT \ln\langle \exp\{-[U(\lambda_{i+1}) - U(\lambda_i)]/kT\}\rangle_i \qquad (1)$$

where $\langle ... \rangle_i$ denotes an isobaric ensemble average for $\lambda = \lambda_i$ and $U(\lambda)$ is the λ-dependent total potential energy. The total free energy change is obtained by summing over all the windows.

2.2. Enthalpy−Entropy Decomposition. The enthalpy change for mutating a solute X into solute Y is

$$\Delta H = \Delta \bar{U} + P\Delta V \qquad (2)$$

where $\Delta \bar{U}$ is the average potential energy change, P is the pressure, and ΔV is the volume change. For the system studied here the $P\Delta V$ term is typically 2 orders of magnitude smaller than $\Delta \bar{U}$ and it will be neglected.

The total potential energy can be subdivided into a solute−solvent term U_{uv}, defined as the interaction energy of the solute with the solvent, and a solvent−solvent term U_{vv}, defined as the sum of the interaction energies of the solvent molecules with all other solvent molecules,

$$U_{vv} = \sum_k \frac{B_k}{2} \qquad (3)$$

where B_k is the solvent binding energy of solvent molecule k, namely the potential energy of solvent molecule k due to all other solvent molecules.

The total average potential energy change $\Delta \bar{U}(i+1, i)$ in the ith window is expressed as the sum of the changes of the

solute−solvent and solvent reorganization energy terms

$$\Delta\bar{U}(i+1, i) = \Delta\bar{U}_{uv}(i+1, i) + \Delta\bar{U}_{vv}(i+1, i) \quad (4)$$

The solute−solvent and solvent−solvent average potential energy changes in the ith window are computed by the thermodynamic perturbation formulas[13,17,23,49,59] expressed as

$$\Delta\bar{U}_{uv}(i+1, i) = \frac{\langle U_{uv}(i+1)\exp[-\Delta U(i+1, i)/kT]\rangle_i}{\langle\exp[-\Delta U(i+1, i)/kT]\rangle_i} - \langle U_{uv}(i)\rangle_i \quad (5)$$

$$\Delta\bar{U}_{vv}(i+1, i) = \frac{\langle\delta U_{vv}\exp[-\Delta U(i+1, i)/kT]\rangle_i}{\langle\exp[-\Delta U(i+1, i)/kT]\rangle_i} \quad (6)$$

where $\Delta U(i+1, i) = U(\lambda_{i+1}) - U(\lambda_i)$, $U_{uv}(i) = U_{uv}(\lambda_i)$, and $\delta U_{vv} = U_{vv} - \langle U_{vv}\rangle_i$ is the instantaneous fluctuation of the solvent−solvent interaction energy. The TP formulas follow from the direct formula[20,35]

$$\Delta\bar{U}(i+1, i) = \langle U(i+1)\rangle_{i+1} - \langle U(i)\rangle_i \quad (7)$$

by evaluating the ensemble average at λ_{i+1} in the ensemble at λ_i employing a standard thermodynamic perturbation approach.

The solute−solvent potential energy change does not present particular computational difficulties. The evaluation of the solvent reorganization energy term, however, is a challenging theoretical and computational problem.

2.2.1. Solvent Reorganization Energy. The calculation of the solvent reorganization energy by means of eq 6 is complicated by the fact that the fluctuations of the term δU_{vv} grows with the number N of solvent molecules as $\sqrt{N}$. This constitutes a formidable obstacle to an accurate estimate of the solvent reorganization energy as the system size increases. The statistical properties of the direct formula

$$\Delta\bar{U}_{vv} = \langle U_{vv}\rangle_Y - \langle U_{vv}\rangle_X \quad (8)$$

have similar characteristics because the fluctuations of the solvent−solvent potential energy grows as $\sqrt{N}$ as well.

The application of the direct formula, by allowing the estimate of the solvent reorganization energy by studying only the end points of the mutation, may be advantageous when the two solutes X and Y are very different. When the two solutes are similar, the thermodynamic perturbation formula eq 6 is preferable because it converges faster than the direct formula eq 8 and can be evaluated in parallel with the free energy without resorting to a separate calculation.

It should be pointed out that the statistical fluctuations of the estimator of the free energy change in eq 1 (when only the solute potential parameters are being mutated) are unaffected by the system size. This accounts for the relatively fast convergence of the free energy compared to the enthalpy and entropy.

2.2.2. Ensemble Dependence. The properties of the solvent reorganization energy under different ensembles have been analyzed.[60,61] It is shown that this term is responsible for the ensemble dependence of the enthalpy and entropy of solvation. Briefly, the enthalpy of solvation for the constant pressure process $(\Delta H)_P$ differs from the energy of solvation at constant volume $(\Delta E)_V$ by a quantity that in the thermodynamic limit is

$$(\Delta H)_P - (\Delta E)_V = \Delta V\frac{T\alpha}{\kappa} \quad (9)$$

where ΔV is the partial molar volume of the solute and α and κ are respectively the thermal expansion coefficient and isothermal compressibility of the pure solvent. The ensemble dependence of the entropy of solvation ($-T\Delta S$), given that the free energy of solvation is ensemble independent, is equal in magnitude but opposite to the ensemble dependence of the enthalpy of solvation given by eq 9. It has been shown[18,47] that the ensemble correction $\Delta VT\alpha/\kappa$, in general, cannot be neglected. It is, in fact, of the same order of magnitude as the enthalpies of solvation of common hydrophobic solutes (for solvation of methane $\Delta VT\alpha/\kappa \simeq 1.5$ kcal/mol) and it increases with solute size. To compare calculated enthalpies and entropies of solvation to experimental measurements that are usually conducted at constant pressure, it is necessary to perform the calculation at constant pressure or, alternatively, apply the correction given in eq 9 to the enthalpy and entropy of solvation obtained at constant volume. Our calculations are performed at constant pressure and can be directly compared to experimental measurements without the need to rely on often approximate estimates of the thermal expansion coefficient and isothermal compressibility of the water model employed.[62]

The ensemble dependence of the solvent reorganization energy does not imply that the solvent reorganizes differently around the solute according to the solute insertion conditions. A careful analysis[18,63,64] shows that the ensemble correction in eq 9 originates from a subtle density-dependent term which scales such as V^{-1} upon insertion of the solute at constant volume. Such bulk response is absent for the solute insertion at constant pressure. In constant pressure simulations, therefore, it is possible to evaluate the solvent reorganization energy by studying only a solvent region close to the solute.

2.2.3. Solvation Shell Approximation. We have adopted a solvation shell approximation[64,65] to perform the enthalpy−entropy decompositions of the free energy of hydration reported in this work. In the solvation shell approximation only the solvent molecules in a region close to the solute are included in the calculation of the solvent reorganization energy.

The accuracy of the solvation shell approximation can be analyzed by comparing the solvent reorganization energy for the insertion of a water molecule in a sample of liquid water to the solvent reorganization energy for the same process calculated in the solvation shell approximation with various solvation shell sizes. This is possible because the solvent reorganization energy as a function of shell size can be obtained very accurately for pure systems using the direct method because each solvent molecule can be, in turn, considered as the solute. The solvent reorganization energy as $N_{shell} \rightarrow \infty$ is exactly minus half the water binding energy.[66]

The solvent reorganization energy at standard conditions as a function of the number N_{shell} of water molecules included in the solvation shell around the water molecule being inserted is shown in Figure 1. It can be observed that a solvation shell composed of a relatively small number of water molecules reproduces quite accurately the total solvent reorganization energy. For the insertion of water into water for example, a solvation shell composed of only 24 water molecules is capable of capturing nearly 90% of the total solvent reorganization energy.

This system also provides a good testing ground for the thermodynamic perturbation formula (eq 6) used to estimate numerically the solvent reorganization energy. Figure 1 shows that the solvent reorganization energy calculated by the thermodynamic perturbation formula (the details of the calculation are described in section 2.5) is in good agreement with the exact

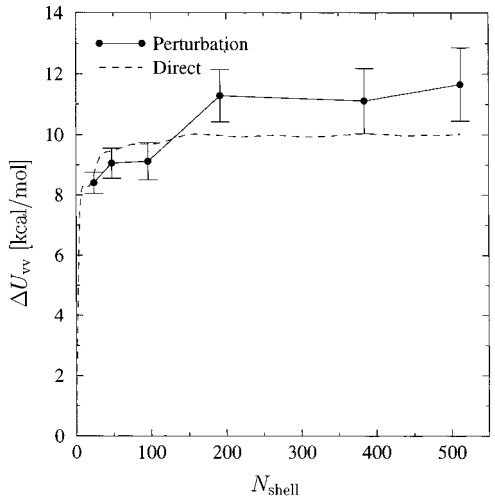

Figure 1. Solvent reorganization energy for inserting a water molecule in water as a function of the number of water molecules in the solvation shell.

result. Overall, the thermodynamic perturbation formula for a solvation shell with only 24 water molecules captures in this case more than 80% of the total solvent reorganization energy. Increasing N_{shell}, however, introduces large statistical and systematic errors. By appropriately reducing the number of solvent molecules included in the solvation shell, one can obtain accurate and reproducible estimates of the solvent reorganization energy.

2.3. Cavity Decomposition. The two main characteristics that determine the solvation properties of hydrophobic species are their size and shape and the magnitude of their attractive interactions with the solvent. The effect of size and shape can be studied independently from the effect of the attractive forces by subdividing the total solvation process into two steps. In the first step a suitable cavity with repulsive walls is created in the solvent. In the second step the molecule is placed in the cavity by adding to the cavity the attractive van der Waals and electrostatic interactions between the solute and the solvent.[12,42−44]

In this work the cavity decomposition is accomplished by decomposing the total solute−solvent site−site interaction potential $u(r)$ into three contributions,

$$u(r) = u_{rep}(r) + u_{vdW}(r) + u_{es}(r) \tag{10}$$

where $u_{rep}(r)$ is a short-ranged repulsive term, $u_{vdW}(r)$ comprises the dispersion van der Waals interactions, and $u_{es}(r)$ is the Coulomb interaction. Details of the forms of these potentials are given in section 2.5. By growing independently the repulsive and attractive terms, the solvation thermodynamics of cavity formation can be isolated from the contributions due to the attractive terms.

2.4. Model. The TIP4P[67] model is used for the water solvent. The water and alkane molecules are considered rigid. All-trans, all-tetrahedral conformations are adopted for linear and branched alkanes, the chair conformation is adopted for cyclohexane, and cyclopentane is prepared in a low-energy puckered conformation. The C−C bond length is 1.53 Å, and the C−H bond length is 1.09 Å throughout.

The electrostatic and van der Waals interactions are modeled according to the OPLS all-atom force field.[68] The atomic partial charges are 0.06 au for all alkyl hydrogen atoms. The atomic partial charge of the methane carbon atom is −0.24 au, and the atomic partial charges of primary, secondary, and tertiary carbon atoms are respectively −0.18, −0.12, and 0.00 au. The Lennard-Jones parameters are $\sigma_{LJ}(C) = 3.5$ Å, $\sigma_{LF}(H) = 2.5$ Å, $\epsilon_{LJ}(C) = 0.066$ kcal/mol, and $\epsilon_{LJ}(H) = 0.03$ kcal/mol.[69]

2.5. Computational Details. The system is composed of 512 water molecules and one solute in a cubic box at 298 K and 1 atm pressure. Periodic boundary conditions and the minimum image convention have been applied in a standard fashion.[70] A sharp molecular cutoff of 12.4 Å has been applied to all pair interactions. System configurations were generated using a constant-pressure Monte Carlo (MC) algorithm.[70] For each (MC) pass 1 attempted move per solvent molecule and 40 attempted moves for the solute were performed. The internal coordinates of the molecules were not sampled. Starting from an fcc ice structure the solution was equilibrated before collecting data.

The FEP calculations were organized as follow. Starting from the pure solvent, a methane molecule was inserted in water using a total of 45 windows. In the first 26 windows a Lennard-Jones particle corresponding to an uncharged carbon atom was created in water; in the following 19 windows the Lennard-Jones particle was mutated into methane. Starting from methane, all the other linear and branched alkanes were created by successive methylations of the existing chain. The FEP calculation of each methylation was performed using 22 windows. Cyclohexane and cyclopentane were created by starting from propane in a sequence of respectively three and two steps with the last one being a ring closure by the insertion of a CH_2 group. Typically, for each window 2000 MC equilibration passes were employed followed by 64 000 MC passes of data acquisition. For the conversion between the alkane and the corresponding repulsive soft cavity 16 FEP windows and 4000 MC passes of averaging per window were employed for each carbon atom. Statistical uncertainties in the averages were estimated by block averaging.[70] The solvation properties of water in water (see section 2.2.3) were obtained by transforming a Lennard-Jones particle corresponding to a carbon atom into a TIP4P water molecule.

The interaction potential parameters are linearly interpolated between the initial and final parameters. For instance, the partial charge on a charged site at λ is given by

$$q(\lambda) = (1 - \lambda)q_i + \lambda q_f \tag{11}$$

where q_i and q_f are the initial and final partial charges at that charged site. A similar approach is adopted for the rigid molecular geometries. If $\{\tilde{\mathbf{R}}_i^{N_a}\}$ and $\{\tilde{\mathbf{R}}_f^{N_a}\}$ are the sets that specify respectively the initial and final molecular geometries in Cartesian atomic coordinates with respect to an arbitrary internal molecular frame, the λ-dependent molecular geometry $\{\tilde{\mathbf{R}}^{N_a}(\lambda)\}$ is given by

$$\{\tilde{\mathbf{R}}^{N_a}(\lambda)\} = (1 - \lambda)\{\tilde{\mathbf{R}}_i^{N_a}\} + \lambda\{\tilde{\mathbf{R}}_f^{N_a}\} \tag{12}$$

For large mutations a linear interpolation approach may lead to very unphysical states along the thermodynamic path. In such cases the mutation from X to Y is better accomplished by a series of such linear interpolations.

The conversion between the alkane and the corresponding repulsive soft cavity is achieved by expressing the Lennard-Jones solute−solvent interaction site−site potentials in the form[71]

$$u_{LJ}(r) = \begin{cases} 4\epsilon\left[\left(\frac{\sigma}{r}\right)^{12} - \left(\frac{\sigma}{r}\right)^{6}\right] + (\epsilon - \epsilon_a) & r < 2^{1/6}\sigma \\ 4\epsilon_a\left[\left(\frac{\sigma}{r}\right)^{12} - \left(\frac{\sigma}{r}\right)^{6}\right] & r > 2^{1/6}\sigma \end{cases} \tag{13}$$

The alkane−solvent LJ interaction is recovered from eq 13 when

TABLE 1: Solvent-Accessible Surface Areas and Solvent-Excluded Volumes of the Alkanes

molecule	SASA (Å^2)	vol (Å^3)
methane	141.196	153.205
ethane	178.472	211.008
propane	209.019	263.157
butane	239.567	315.307
pentane	270.115	367.456
hexane	300.662	419.606
isobutane	233.919	310.175
2-methylbutane	257.991	354.355
neopentane	254.007	352.657
cyclopentane	244.941	329.281
cyclohexane	262.341	365.684

the attractive well depth ϵ_a is equal to the LJ well depth ϵ. The conversion between the alkane and the corresponding repulsive soft cavity is carried out by varying ϵ_a from ϵ to zero and simultaneously setting all the charges to zero.

The free energy changes were obtained from the FEP formula eq 1, and the solute−solvent energy change is calculated by eq 5. For the calculation of the solvent reorganization energy, the solvation shell around the solute is defined to be composed of the N_{shell} solvent molecules closest to a chosen atomic site of the solute.[72] For the annihilation of water (Figure 1) this site is the oxygen atom, and the carbon atom is the site for the annihilation of methane. For the methylations, the atomic site at the center of the solvation shell was the carbon atom being methylated. The transformation of a molecule in its corresponding soft repulsive cavity is carried out one carbon group at a time, and the solvation shell center is the carbon atom itself. The solvation shell approximation of the solvent reorganization energy is then obtained from eq 6 where in the expression (3) for U_{vv} only the molecules currently in the solvation shell are included. The values reported here for the solvent reorganization energy have been obtained by setting $N_{shell} = 24$ that, as has been already shown, gives accurate results for the insertion of water in water. No attempt was made to optimize N_{shell} with respect to the experimental hydration enthalpies of the alkanes.

The solvent accessible surface areas (SASA) of the alkanes are obtained using the algorithm by Connolly.[73,74] The solvent-excluded volume of the solute is composed of exclusion spheres centered on each solute atom. The radii of the excluded sphere have been estimated from the continuous solute−water Lennard-Jones interactions by calculating the thermal radius of the repulsive portion of the LJ potential

$$u_{rep}(r) = \begin{cases} 4\epsilon\left[\left(\frac{\sigma}{r}\right)^{12} - \left(\frac{\sigma}{r}\right)^{6}\right] + \epsilon & r < 2^{1/6}\sigma \\ 0 & \text{otherwise} \end{cases} \quad (14)$$

where $\sigma = (\sigma_i\sigma_O)^{1/2}$ and $\epsilon = (\epsilon_i\epsilon_O)^{1/2}$, σ_i and ϵ_i refer the LJ parameters of either carbon or hydrogen, and σ_O and ϵ_O refer to the LJ parameters of the water oxygen. The thermal radius is defined as the distance at which the interaction potential is equal to kT. The thermal radii for the carbon−water and hydrogen-water pairs calculated in this fashion are respectively 3.038 and 2.507 Å. The resulting accessible surface areas and volumes are reported in Table 1.

Results and Discussion

3.1. Free Energies, Enthalpies, and Entropies of Hydration: Experiments and Calculations. The experimental free energies, enthalpies, and entropies of hydration of the alkanes studied are shown in Figure 2. The striking feature is that the entropic and enthalpic terms are significantly larger in absolute value than the hydration free energies. The hydration enthalpies

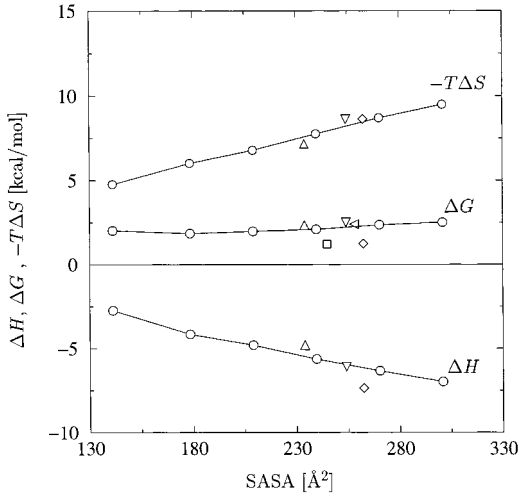

Figure 2. Experimental alkane free energies, enthalpies, and entropies of hydration: (○) normal alkanes from C_1 to C_6 in order of increasing surface area; (△) isobutane; (rotated triangle) 2-methylbutane; (▽) neopentane; (□) cyclopentane; (◇) cyclohexane.

are large and favorable, and the hydration entropies are large and unfavorable. The entropic terms are marginally larger in absolute value than the enthalpic terms resulting in the unfavorable but small hydration free energies of the alkanes. It is recognized that this behavior is typical of hydrophobic hydration. Solvation of apolar compounds in most other solvents, in fact, is usually accompanied by smaller enthalpic and entropic changes.[75]

The calculated free energies, enthalpies, and entropies of hydration of the normal alkanes from methane to hexane, of the branched alkanes 2-methylpropane, 2-methylbutane, and neopentane, and of the cyclic alkanes cyclopentane and cyclohexane are shown in Table 2. The calculated and experimental data are plotted in Figures 3−5 with respect to the solvent-accessible surface area (SASA). The SASA is a commonly used predictor of the hydration properties of nonpolar compounds;[31] it is used here as a reference to discuss the observed trends of the experimental and calculated data. In Figures 3−5, the calculated values are expressed relative to experimental free energy, enthalpy, and entropy of methane.

In general, the calculated and experimental values are in good agreement. The model reproduces most of the main characteristics of the hydration thermodynamics of the alkanes. In the rest of this section we discuss in detail the comparison between the experimental measurements and the results of the calculations. The ability to compare, in addition to the free energy, the calculated enthalpies and entropies of hydration to the experiments is very useful in formulating a way to modify the force field parameters in order to improve the agreement between the experimental and calculated quantities. Indeed, by observing that the entropy of hydration is mainly determined by the size of the alkane whereas the magnitude of the solute−solvent interactions primarily affects only the enthalpy of hydration, we are able to suggest specific modifications of the model parameters to improve the accuracy of the model.

The calculated hydration free energy of methane is 20% more positive than the experimental methane hydration free energy (2.00 kcal/mol). This discrepancy is partly due to the fact that the calculated hydration enthalpy of methane is about 0.8 kcal/mol less negative than the experiments (−2.75 kcal/mol). This represents a significant discrepancy if compared to the good agreement between the calculated and experimental relative hydration enthalpies for the higher alkanes. The calculated

TABLE 2: Calculated Hydration Free Energies (ΔG), Enthalpies (ΔH), Entropies ($-T\Delta S$), Solute−Solvent Energies (ΔU_{uv}), Solvent Reorganization Energy Changes (ΔU_{vv}), and Solute−Solvent Contribution of the Hydration Entropies ($-T\Delta S_{uv}$) of the Alkanes[a]

molecule	ΔG	ΔH	$-T\Delta S$	ΔU_{uv}	ΔU_{vv}	$-T\Delta S_{uv}$
methane	2.404 ± 0.042	−1.991 ± 0.189	4.395 ± 0.194	−3.313 ± 0.024	1.322 ± 0.188	5.717 ± 0.048
ethane	2.630 ± 0.047	−3.153 ± 0.207	5.783 ± 0.212	−5.437 ± 0.025	2.284 ± 0.205	8.067 ± 0.053
propane	2.890 ± 0.051	−3.895 ± 0.234	6.786 ± 0.240	−7.209 ± 0.030	3.314 ± 0.232	10.099 ± 0.059
butane	3.210 ± 0.055	−4.399 ± 0.256	7.608 ± 0.262	−8.977 ± 0.033	4.579 ± 0.254	12.187 ± 0.064
pentane	3.447 ± 0.058	−5.351 ± 0.274	8.798 ± 0.281	−10.774 ± 0.036	5.423 ± 0.272	14.221 ± 0.068
hexane	3.781 ± 0.064	−5.682 ± 0.299	9.462 ± 0.306	−12.384 ± 0.040	6.703 ± 0.296	16.165 ± 0.075
isobutane	3.029 ± 0.055	−4.233 ± 0.254	7.262 ± 0.260	−8.883 ± 0.033	4.650 ± 0.252	11.912 ± 0.064
2-methylbutane	3.510 ± 0.059	−4.704 ± 0.272	8.213 ± 0.278	−10.130 ± 0.037	5.426 ± 0.269	13.640 ± 0.069
neopentane	3.234 ± 0.061	−5.089 ± 0.283	8.323 ± 0.290	−10.387 ± 0.039	5.297 ± 0.280	13.621 ± 0.072
cyclopentane	2.802 ± 0.058	−5.056 ± 0.264	7.858 ± 0.270	−9.983 ± 0.037	4.928 ± 0.261	12.785 ± 0.068
cyclohexane	2.338 ± 0.060	−6.668 ± 0.281	9.006 ± 0.287	−11.662 ± 0.039	4.994 ± 0.278	14.000 ± 0.071

[a] Values reported in kcal/mol at 298 K.

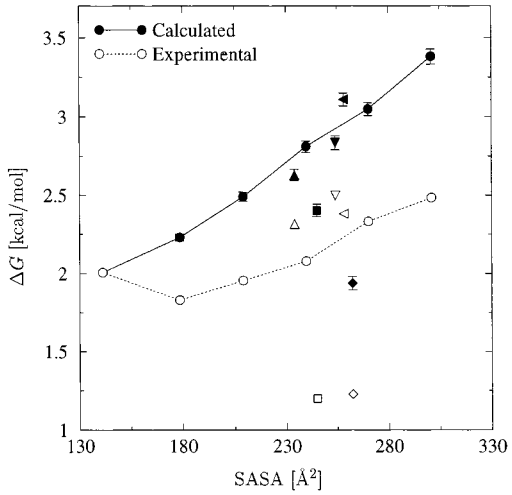

Figure 3. Calculated and experimental[93] hydration free energies of the alkanes vs their solvent accessible surface area (SASA). Calculated free energies are shown taking as a reference the experimental hydration free energy of methane. Calculated values are represented with filled symbols, and experimental measurements, by open symbols: (○) normal alkanes from C_1 to C_6 in order of increasing surface area; (△) isobutane, (rotated triangle) 2-methylbutane; (▽) neopentane, (□) cyclopentane; (◇) cyclohexane.

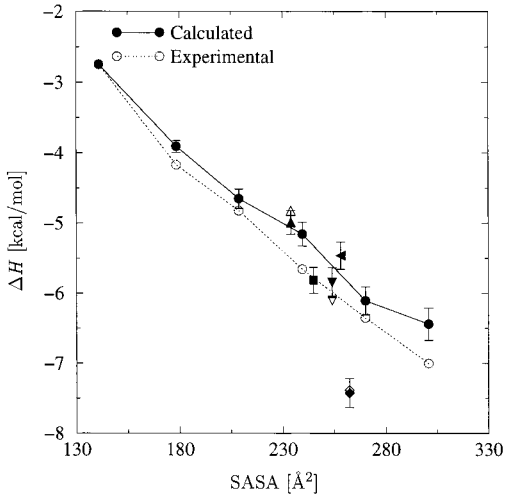

Figure 4. Calculated and experimental[93] hydration enthalpies of the alkanes vs their solvent accessible surface area (SASA). Calculated enthalpies are shown taking as a reference the experimental hydration enthalpy of methane. See Figure 3 for the symbol keys. The standard state conversion factor 0.549 kcal/mol = $-RT(1 - T\alpha_{water})$ has been added to the experimental values of ΔH given in ref 93.

hydration entropy of methane, although in better agreement with the experimental hydration entropy ($-T\Delta S = 4.75$ kcal/mol), is found to be too small. The discrepancies in the enthalpy and entropy partially cancel each other resulting in a smaller discrepancy in the free energy. The data suggest that the model could be improved by increasing the methane-excluded volume while keeping the dispersion van der Waals water−methane interactions per unit surface area approximately constant. These modifications will increase the hydration entropy loss and also increase the solvent-accessible area of methane resulting in a stronger solute−solvent interaction. Both effects together would move the calculated hydration properties toward the experimental values. These force field modifications could then be propagated almost unchanged to all the other alkanes as the enthalpies and entropies of the larger alkanes relative to methane are in fairly good agreement with the experiments.

The calculated and experimental hydration free energies of the alkanes are positive and generally increase with increasing solvent accessible surface area (Figure 3). Experimentally, however, it is observed that the hydration free energy of ethane is smaller than the hydration free energy of methane. The drop in free energy of hydration in going from methane to ethane is not reproduced by the calculations. [A previous calculation,[40] which reproduces the larger solubility of ethane with respect to methane, was later found to be not fully converged.[76]] The calculations underestimate the magnitude of the negative enthalpy change and overestimate the entropy loss in going from methane to ethane. Both effects contribute to a less favorable hydration free energy of ethane. It appears, therefore, that the current alkane model should allow for a larger gain in favorable alkane−water interactions in going from methane to ethane without further entropy loss. This could be achieved by increasing the ethane−water Lennard-Jones interaction parameters and, given the strong dependency of the hydration entropy on molecular size discussed below, by decreasing the ethane/methane size ratio in water.

The experiments also show that each methylation beyond the first increases the free energy of hydration of the linear alkanes by approximately 0.2 kcal/mol whereas the calculated free energy increase at each methylation is on average slightly higher.

The calculations reproduce very well the experimental 1.2 kcal/mol free energy difference between hexane and cyclohexane. For cyclopentane the calculations predict a free energy of hydration that is only ≃0.6 kcal/mol smaller than the hydration free energy of pentane, while experimentally this free energy difference is about 1.1 kcal/mol.

The calculated and experimental enthalpies of hydration of the normal alkanes are in good agreement (Figure 4). This level of agreement could not have been achieved by ignoring the solvent reorganization energies. Each CH_2 group contributes

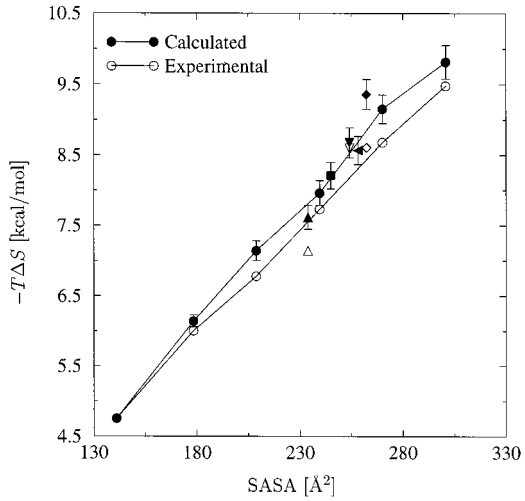

Figure 5. Calculated and experimental[93] hydration entropies ($-T\Delta S$) of the alkanes vs their solvent accessible surface area (SASA). Calculated entropies are shown taking as a reference the experimental hydration entropy of methane. See Figure 3 for the symbol keys. The standard state conversion factor 0.549 kcal/mol $= -RT(1 - T\alpha_{water})$ has been subtracted from the values of the experimental values of $-T\Delta S$ given in ref 93.

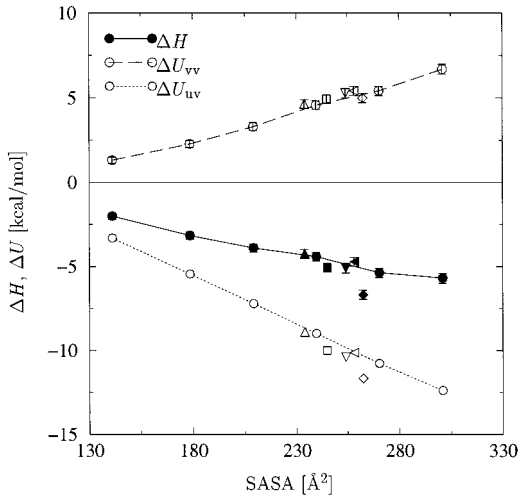

Figure 6. Enthalpies (ΔH), solute−solvent energies (ΔU_{uv}), and, in the upper portion of the figure, solvent reorganization energies (ΔU_{uv}) of the alkanes vs their solvent accessible surface area (SASA). See Figure 3 for the symbol keys.

roughly −0.6 kcal/mol to the enthalpy of hydration. The calculations slightly underestimate the magnitude of the experimental enthalpies of hydration. Despite the quite favorable enthalpies of hydration, the solubility in water of these compounds remains low due to the unfavorable entropies.

Calculated and experimental entropies of hydration of the linear alkanes are also in good agreement (Figure 5). The experimental entropy losses, however, are overestimated by the calculations. This effect could be in partly due to having ignored the torsional degrees of freedom of the carbon chains. For linear alkanes each additional methylation decreases $T\Delta S$ by about 0.8 kcal/mol. The $T\Delta S$ values are larger in magnitude than the ΔH values resulting in the positive hydration free energies discussed above.

The alkane hydration free energies result from a large cancellation between enthalpic and entropic components. The ΔH and $T\Delta S$ values are each 3−4 times larger in magnitude than the free energies. Subtle variations of the entropies and enthalpies of hydration are, in fact, the cause of the anomalies in the trend of hydration free energies, for example the slight decrease in going from methane to ethane (not observed in the calculations) and the surprisingly high solubilities of the cyclic alkanes.

Experimentally, the hydration free energies per unit surface area of the branched alkanes are slightly more positive than their linear counterparts. For isobutane this effect is caused by a less favorable enthalpy of hydration only partially offset by a smaller entropic loss. In contrast, the low solubility of neopentane is due to a larger entropic penalty than the corresponding linear homologues (see Figure 5). The calculated hydration enthalpies per unit surface area are consistently less favorable, and the entropy loss per unit surface area are smaller than the corresponding linear molecules. The calculations are successful in reproducing qualitatively the experimentally observed hydration entropy and enthalpy of isobutane; the agreement, however, is not quantitative, and the lower relative solubility of isobutane is not accurately reproduced. For neopentane the disagreement with the experiments is of a qualitative nature. The hydration free energy of neopentane is predicted to be roughly equal, as opposed to lower, than a linear alkane of the same solvent accessible surface area, and the ordering of the hydration enthalpy and entropy is reversed with respect to the experiments.

The free energies of hydration of the cyclic alkanes favor hydration more than their corresponding linear homologues. The free energy drop caused by cyclization is reproduced by the calculations, although underestimated in the case of cyclopentane. Both experimentally and computationally, the larger than predicted solubility of cyclohexane compared to hexane is mostly attributed to the significantly more favorable than expected enthalpy of hydration. Despite their different accessible surface areas, in fact, the enthalpies of cyclohexane and hexane are of similar magnitude. The calculations also show that the larger solubility of cyclopentane compared to an alkane of the same solvent accessible surface area is due mostly to a more favorable hydration enthalpy, although partially offset by a more unfavorable entropic component.

3.2. Solute−Solvent Energy, Solvent Reorganization Energy, and Enthalpy−Entropy Compensation. As described in section 2.2.1, we have computed separately the solute−solvent energy and the solvent reorganization contributions to the enthalpy of hydration. These contributions provide insights into the thermodynamics of solvation, and we will use them to discuss the observed enthalpies of hydration. Table 2 and Figure 6 show the results of this decomposition for the alkanes examined.

In general the solute−solvent interaction energies are large and negative, steadily decreasing by about −1.8 kcal/mol for each methylation. With about −12 kcal/mol, hexane has, in absolute value, the largest interaction energy with water in this alkane set. In contrast, the total enthalpy of hydration decreases by only −0.6 kcal/mol for each methylation and for hexane is only −4.8 kcal/mol. This is due to the solvent reorganization component which is positive and steadily increases after each methylation. The solvent reorganization energy is, in absolute value, smaller than the solute−solvent interaction energy, but it is far from negligible as it comprises as much as 40% of the total hydration enthalpy. Satisfactory agreement with the experimental enthalpies of hydration, therefore, can only be achieved by taking into consideration the solvent reorganization energies.

The enthalpy of hydration is the result of a cancellation between the larger and negative solute−solvent interaction energy and the solvent reorganization energy which is of smaller

magnitude and positive. The correlation between solute−solvent and solvent reorganization energies can be rationalized by observing that in this system the magnitude of the interaction of the solute with the water molecules increases with increasing solute size. In turn, the larger the solute, the more extensive the solvent structure disruption that is ultimately manifested in the unfavorable solvent reorganization energy.

As we have pointed out in the previous section, the experimental data and the calculations show that the higher than expected solubility of cyclohexane is mostly an enthalpic phenomenon. Moreover, Figure 6 shows that the larger than expected favorable enthalpy of hydration of cyclohexane compared to the linear alkanes is largely due to the strong cyclohexane−water interactions. Indeed, the solute−solvent energy per unit surface area for cyclohexane is more negative than for the linear alkanes, whereas the solvent reorganization energy per unit surface area is constant for all the alkanes examined (roughly 34 cal/mol Å^2). The same considerations seem to apply, but to a smaller degree, to cyclopentane and the branched alkanes. These observations suggest that, despite their larger solvent accessible surface area, linear alkanes are unable to form interaction contacts with a proportionally larger number of solvent molecules. Due to the close packing of the solvating water molecules, additional water molecules are prevented from entering the first solvation shell unless the accessible surface area of the solute increases by a minimum increment. This effect is due to the finite size of the water molecules and cannot be easily captured by implicit solvation parameters such as the accessible surface area.

In conclusion, the larger solubility of cyclohexane with respect to hexane is explained by observing that in going from hexane to cyclohexane (i) the unfavorable entropy and solvent reorganization energy decrease roughly proportionally to the decrease in solvent accessible surface area and (ii) the magnitude of the favorable solute−solvent energy decreases to a much smaller degree than expected from the loss of solvent accessible surface area and of two interaction centers (two hydrogen atoms).

The solvent reorganization model[77,78] is sometimes invoked to explain the often observed phenomenon of entropy−enthalpy compensation,[13,47,49] expressed as

$$|\Delta H|, |T\Delta S| > |\Delta G| \tag{15}$$

whereby entropy and enthalpy variations partially cancel each other to yield a smaller free energy change. In the solvent reorganization model, the enthalpy and entropy changes are, ignoring the $P\Delta V$ term, decomposed as follows:[17,80]

$$\Delta H = \Delta \bar{U}_{uv} + \Delta \bar{U}_{vv} \tag{16}$$

$$-T\Delta S = -T\Delta S_{uv} - \Delta \bar{U}_{vv} \tag{17}$$

where $\Delta \bar{U}_{uv}$ is the solute−solvent average potential energy change, $\Delta \bar{U}_{vv}$ is the solvent reorganization energy, and $-T\Delta S_{uv}$ is a quantity, defined by eq 17, which is referred to as the solute−solvent entropy change. When the free energy is obtained by summing eqs 16 and 17

$$\Delta G = \Delta U_{uv} - T\Delta S_{uv} \tag{18}$$

the solvent reorganization term cancels out and it does not contribute to the free energy change. The solvent reorganization model, therefore, predicts that the larger the solvent reorganization energy, the more likely is the occurrence of entropy−enthalpy compensation.

The solvent reorganization model is useful in predicting entropy−enthalpy compensation in the following two cases: (i) The solvent reorganization energy term is larger in absolute value than $|\Delta U_{uv}|$ and $|T\Delta S_{uv}|$. In this case entropy−enthalpy compensation will necessarily occur. (ii) The quantities ΔU_{uv} and $T\Delta S_{uv}$ over a series of solutes are uncorrelated from each other. In this case (and if condition 1 is not met) the occurrence of entropy−enthalpy compensation will be, in a statistical sense, more likely than entropy−enthalpy reinforcement.

For the hydration of hydrocarbons, the data presented here show, however, that none of the above conditions are satisfied. Table 2 clearly shows that the solvent reorganization energy is always smaller in absolute value than the solute−solvent potential energy term and the solute−solvent entropy term. Moreover, the values of ΔU_{uv} and $-T\Delta S_{uv}$ are far from being uncorrelated. In fact, they always oppose each other and grow roughly proportionally to alkane size. Additionally, by subtraction of the solvent reorganization energy from ΔH and $T\Delta S$, the remainders that are produced (the solute−solvent term and solute−solvent entropy term) are even larger in absolute value than the original ΔH and $T\Delta S$ values. These remainders, therefore, compensate each other even more strongly than ΔH and $-T\Delta S$. It appears, therefore, that in this case the solvent reorganization decomposition expressed by eqs 16 and 17 instead of clarifying the causes of entropy−enthalpy compensation introduces terms whose entropy−enthalpy compensation analysis is even more difficult to justify. The analysis of the data obtained in the present study shows that it is the compensation between ΔU_{uv} and $-T\Delta S_{uv}$ that ultimately provides the basis for entropy−enthalpy compensation that is observed in the solubilities of the hydrocarbons in water.

3.3. Cavity Decomposition. The study of the solvation thermodynamics of cavity formation is of a particular importance because it is thought to form the basis for hydrophobic hydration.[19,42,46,51,81] The probability of the natural occurrence of a suitable void of solvent molecules in a liquid determines the free energy of hydration of a repulsive cavity.[44,46,82−84] In liquid water, given the small size of a water molecule and the close-packing structure, the occurrence of a large solvent void is extremely unlikely. By analogy with hard sphere fluids, it is thought that the unfavorable free energy of hydration of a repulsive cavity is entropy dominated; formation of the cavity causes loss of translational and rotational entropy of the liquid. The magnitude of the water reorganization energy near a repulsive cavity is, however, also important.[51] We will show, in fact, that in the systems studied the solvent reorganization energy for cavity hydration accounts for as much as 50% of the cavity hydration free energy.

Cavity hydration can be studied by monitoring the probability of the natural occurrence of a void in a sample of pure solvent.[44,82,83,85] Pratt et al.[46,86] obtained the average and variance of the number of solvent molecules in a certain volume and used information theory techniques to predict the probability that no water molecules are present in the volume. In the present work the alkane cavities are constructed from the corresponding alkanes by removing the atomic partial charges and the attractive solute−solvent van der Waals interactions. In the next section we will provide numerical comparisons between the calculated free energy of alkane cavity hydration and the information theory predictions for the same cavities.

The hydration thermodynamic properties of the alkane cavities examined in this work are reported in Table 3. In Table 4 we report the changes relative to the mutation of the alkane cavities to the corresponding alkanes. The latter corresponds to the

TABLE 3: Calculated Hydration Free Energies (ΔG), Enthalpies (ΔH), Entropies ($-T\Delta S$), Solute−Solvent Energy Changes (ΔU_{uv}), and Solvent Reorganization Energies (ΔU_{vv}) of the Alkane Cavities[a]

molecule	ΔG	ΔH	$-T\Delta S$	ΔU_{uv}	ΔU_{vv}
methane	6.721 ± 0.044	3.290 ± 0.192	3.431 ± 0.197	0.963 ± 0.028	2.327 ± 0.190
ethane	8.926 ± 0.048	3.896 ± 0.213	5.030 ± 0.218	0.854 ± 0.029	3.042 ± 0.211
propane	11.421 ± 0.054	5.951 ± 0.243	5.470 ± 0.249	1.241 ± 0.035	4.711 ± 0.240
butane	13.374 ± 0.058	7.432 ± 0.266	5.942 ± 0.272	1.173 ± 0.039	6.260 ± 0.263
pentane	15.511 ± 0.063	9.472 ± 0.285	6.039 ± 0.292	1.259 ± 0.044	8.213 ± 0.282
hexane	18.037 ± 0.069	10.487 ± 0.310	7.550 ± 0.318	1.850 ± 0.048	8.636 ± 0.307
isobutane	13.112 ± 0.059	7.811 ± 0.262	5.300 ± 0.269	1.139 ± 0.040	6.672 ± 0.259
2-methylbutane	15.626 ± 0.063	9.266 ± 0.281	6.360 ± 0.288	1.952 ± 0.043	7.315 ± 0.278
neopentane	15.189 ± 0.063	8.103 ± 0.293	7.087 ± 0.299	1.504 ± 0.042	6.599 ± 0.290
cyclopentane	14.390 ± 0.060	8.760 ± 0.276	5.629 ± 0.282	1.614 ± 0.042	7.147 ± 0.273
cyclohexane	15.731 ± 0.063	8.716 ± 0.292	7.015 ± 0.298	1.655 ± 0.044	7.061 ± 0.288

[a] Values reported in kcal/mol at 298 K.

TABLE 4: Calculated Free Energies (ΔG), Enthalpies (ΔH), Entropies ($-T\Delta S$), Solute−Solvent Energy Changes (ΔU_{uv}), and Solvent Reorganization Energies (ΔU_{vv}) for the Process of Adding the Attractive Interactions to the Repulsive Potential of the Alkane Cavities[a]

molecule	ΔG	ΔH	$-T\Delta S$	ΔU_{uv}	ΔU_{vv}
methane	−4.317 ± 0.015	−5.281 ± 0.028	0.964 ± 0.032	−4.276 ± 0.015	−1.005 ± 0.024
ethane	−6.296 ± 0.013	−7.049 ± 0.052	0.753 ± 0.054	−6.291 ± 0.014	−0.758 ± 0.051
propane	−8.531 ± 0.017	−9.847 ± 0.063	1.316 ± 0.066	−8.450 ± 0.018	−1.397 ± 0.061
butane	−10.165 ± 0.019	−11.831 ± 0.071	1.666 ± 0.073	−10.150 ± 0.020	−1.681 ± 0.068
pentane	−12.064 ± 0.023	−14.823 ± 0.077	2.760 ± 0.081	−12.033 ± 0.024	−2.791 ± 0.073
hexane	−14.256 ± 0.026	−16.168 ± 0.083	1.912 ± 0.087	−14.234 ± 0.028	−1.934 ± 0.078
isobutane	−10.083 ± 0.022	−12.044 ± 0.065	1.962 ± 0.068	−10.022 ± 0.022	−2.022 ± 0.061
2-methylbutane	−12.117 ± 0.022	−13.970 ± 0.071	1.854 ± 0.074	−12.082 ± 0.023	−1.889 ± 0.067
neopentane	−11.955 ± 0.016	−13.192 ± 0.075	1.237 ± 0.077	−11.891 ± 0.017	−1.301 ± 0.073
cyclopentane	−11.588 ± 0.019	−13.816 ± 0.080	2.229 ± 0.083	−11.597 ± 0.020	−2.219 ± 0.078
cyclohexane	−13.393 ± 0.019	−15.384 ± 0.079	1.991 ± 0.081	−13.317 ± 0.020	−2.067 ± 0.076

[a] Values reported in kcal/mol at 298 K.

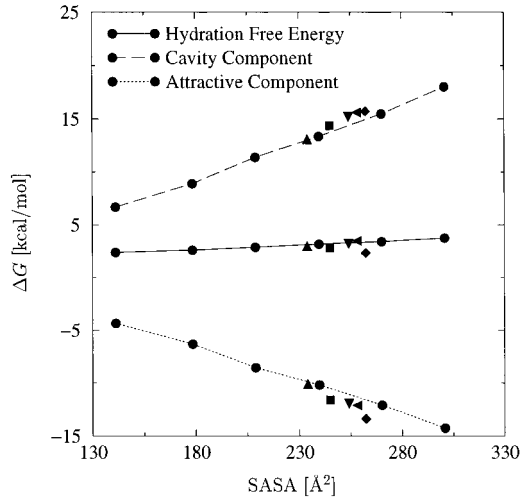

Figure 7. Cavity and van der Waals attraction decomposition of the alkanes hydration free energies shown vs their solvent-accessible surface area (SASA). See Figure 3 for the symbol keys.

process of reestablishing the full alkane−water potential by adding the attractive Lennard-Jones and electrostatic interactions to the repulsive potential of the cavities.

Figure 7 illustrates the decomposition of the hydration free energies of the alkanes into the free energy of cavity hydration plus the free energy changes due to forming the attractive van der Waals and electrostatic interactions. The cavity and attractive components are much larger in magnitude than the hydration free energies. The cavity component is large and positive while the attractive component is large and negative. The attractive component is slightly smaller in magnitude than the cavity component resulting in the positive but small alkane hydration free energies. The hydration free energies are, thus, the result of a large cancellation between the large reversible work needed to create the cavity in water and the large reversible work released when the dispersion interactions between the solute and water are turned on.

Branched and cyclic alkanes have slightly larger than expected cavity hydration free energies than the linear alkanes. The magnitudes of the dispersion free energies of the branched and cyclic alkanes are, in absolute value, also larger than expected. Moreover, these two terms do not cancel each other in a predictable manner resulting in the complex pattern of calculated solubilities of the branched alkanes discussed previously. The cavity decomposition of the hydration free energies is unable to present a clear explanation for the smaller than expected solubilities of the branched alkanes. For these molecules, however, even the experimental evidence on the enthalpies and entropies of hydration suggests that the effects involved are subtle and difficult to predict.

The cavity decomposition for the cyclic alkanes, in contrast, clearly indicates that their larger than expected water solubilities are due to a more favorable then expected dispersion component that, as shown below, is dominated by the favorable solute−solvent interaction energies. Although the work required to create the cavities of the cyclic alkanes is slightly larger than expected, the cyclic alkanes are more soluble due to their dispersion hydration free energies, which are significantly more favorable then the SASA predictions.

The cavity free energies are linearly correlated with the solvent-accessible surface area much better than the total hydration free energies. We attribute the deviations from linearity of the alkane hydration free energies to the complex behavior of the dispersion free energy component. While these deviations are small compared to the large magnitudes of the cavity and attractive free energies, they are quite significant compared to the small total free energies of hydration. This

reflects the very large cancellation between the repulsive cavity and attractive components.

In Table 3 we also report the entropy−enthalpy decomposition of the cavity hydration free energies. As the solvation of a hard sphere solute in a hard sphere solvent is exclusively an entropic process, it is surprising to observe that the enthalpy of cavity hydration is generally larger than the corresponding entropy term. In water the hydration free energy of the alkane cavities appears to be enthalpy dominated. This phenomenon is not due to the "softness" of the cavities considered in this work, as it can be observed that the solute−solvent component of the enthalpy is very small compared to the solvent reorganization energy. The enthalpy of cavity hydration is, thus, largely due to the water reorganization energy.

It can be also observed that, unlike many other thermodynamic processes, the enthalpy and entropy of cavity hydration do not cancel each other. Cavity hydration is unfavorable both enthalpically and entropically. This anomalous phenomenon can be explained by the fact that, even though the magnitude of the interactions between water molecules around the cavity is decreased, the solvent loses translational and rotational entropy due to the presence of the solute cavity which makes the solution no longer homogeneous and isotropic.

We have observed that the entropy of hydration of both nonpolar and polar compounds is mainly determined by the entropy of their associated cavity. Indeed, the process of turning on the solute−solvent van der Waals and electrostatic interactions for the species we have examined (alkanes, water, and amines[87]) is usually accompanied by relatively small entropy changes.

From Table 4 we observe that the process of adding the attractive Lennard-Jones interactions to the repulsive potential of the cavities is enthalpy dominated. The entropy changes are small, and the free energy changes are dominated by the enthalpy changes. A closer examination reveals that most of the enthalpy changes are due to the increase in magnitude of the attractive solute−solvent interactions whereas the solvent reorganization energy changes are small. Note also that the entropy changes, although small, are almost exactly counterbalanced by the solvent reorganization energies. This effect, as predicted by Lee,[51] occurs whenever the fluctuation of the solute−solvent energy change is small. From these observations we conclude that, although the magnitude of the solute−solvent interaction changes considerably, the process of adding the attractive interaction terms involves little structural rearrangements. The numerical results shown in Table 4 are consistent with the liquid state model which forms the basis for the Weeks−Chandler−Andersen (WCA) theory,[71] according to which the equilibrium structure of an apolar liquid is determined largely by the volume and shape of the impenetrable molecular cores and only secondarily by the van der Waals interactions. Apparently, this idea also applies very well to the structure of a solution of an apolar compound in water where solute−solvent electrostatic interactions are small, as originally suggested by Pratt and Chandler.[42]

The decomposition of the alkane hydration process into the formation of an alkane cavity followed by the addition of the attractive solute−solvent interactions shows that, because of the significant solvent reorganization energy, the first process is not purely entropic, as would be expected for a hard sphere solvent. The second process, in contrast, is nearly totally enthalpic; to a good approximation the attractive van der Waals interactions only rescale the solute−solvent potential energy without affecting the solution structure. This suggests that in certain limits it is possible to parametrize molecular force fields for liquid simulations by varying independently parameters that define the size of molecules, which largely determine the liquid structure and parameters that measure the attractive interactions between the molecules, which determine the energy of the system.

Moreover, the analysis of the data collected suggests a means to develop an empirical parametrization model aimed at estimating hydrophobic hydration free energies. Existing models commonly aggregate the cavity and van der Waals contribution in a single nonpolar contribution that is parametrized via the solvent-accessible surface area of the molecule.[30,88,89] However when using a microscopic water surface tension obtained by fitting the experimental hydration free energies of the linear alkanes,[31,90] this technique presents some drawbacks as, for examples, it fails to predict accurately the free energy of hydration of the cyclic alkanes. We observe that the strong correlation between the cavity hydration free energies and the solute surface area makes it easy to predict the properties of molecular cavities of a large variety of compounds. In contrast, the dispersion properties appear to be much more specific to each compound. It may, therefore, prove useful to separate the total hydrophobic hydration free energy into cavity and dispersion contributions. A parametrization of hydration free energies should then include contributions from these two components. However, it is probably not desirable to separately fit each contribution because the large numerical cancellation between the two terms in the free energy would require each term to be fit with extremely high accuracy. We are pursuing an alternative approach which involves a two-term simultaneous fit of the hydration free energies for which correlation between the parameters is anticipated.

3.4. Conformational Dependence of the Thermodynamics of Apolar Hydration. In the previous section it was shown that for the linear and cyclic alkanes the cavity hydration free energies are linearly correlated with the solvent accessible surface area. In contrast, the van der Waals dispersion free energies appear to be strongly correlated with the atomic composition of the molecule and weakly correlated with the SASA. It is difficult to unambiguously confirm this hypothesis from the data collected so far because all the structures examined differ from each other by atomic composition, and topology, in addition to SASA. One way to separate composition from SASA effects is to study different conformations of the same molecule in order to vary the SASA keeping the same atomic composition and connectivity. Toward this end, we have examined the hydration thermodynamics of the ttt, tgt, tgg, and ggg rotamers of *n*-hexane. The nomenclature refers to the trans (t) or gauche (g) conformation of the carbon chain around respectively the 2−3, 3−4, and 4−5 C−C bonds. The ttt rotamers is the all-*trans*-*n*-hexane conformation analyzed in the previous sections. The ggg rotamer is identical to cyclohexane apart from the presence of two additional hydrogens along the 1−6 C−C bond.

Table 5 reports the calculated free energies, enthalpies, and entropies of hydration of the hexane rotamers. The solute−solvent and solvent reorganization energy components of the hydration enthalpy are also reported in Table 5. Figure 8 shows the hydration free energies of the hexane rotamers compared to the hydration free energies of the alkanes from Figure 3. The hydration free energies of the hexane rotamers decrease rapidly with decreasing SASA. The ggg hexane rotamer is predicted to be even more soluble that cyclohexane due to the favorable solute−solvent energy provided by the two additional hydrogens. It was verified that by removing the two additional

TABLE 5: Calculated Hydration Free Energies (ΔG), Enthalpies (ΔH), Entropies ($-T\Delta S$), Solute−Solvent Energy Changes (ΔU_{uv}), and Solvent Reorganization Energies (ΔU_{vv}) of the Hexane Rotamers[a]

molecule	ΔG	ΔH	$-T\Delta S$	ΔU_{uv}	ΔU_{vv}
hexane (ttt)	3.781 ± 0.064	−5.682 ± 0.299	9.462 ± 0.306	−12.384 ± 0.040	6.703 ± 0.296
hexane (tgt)	3.386 ± 0.085	−4.708 ± 0.403	8.094 ± 0.412	−12.192 ± 0.063	7.484 ± 0.398
hexane (tgg)	2.600 ± 0.098	−5.175 ± 0.480	7.775 ± 0.490	−12.214 ± 0.078	7.039 ± 0.474
hexane (ggg)	1.099 ± 0.117	−5.879 ± 0.578	6.979 ± 0.590	−12.295 ± 0.095	6.416 ± 0.570

[a] Values reported in kcal/mol at 298 K.

TABLE 6: Calculated Hydration Free Energies (ΔG), Enthalpies (ΔH), Entropies ($-T\Delta S$), Solute−Solvent Energy Changes (ΔU_{uv}) and Solvent Reorganization Energies (ΔU_{vv}) of the Hexane Rotamer Cavities[a]

molecule	ΔG	ΔH	$-T\Delta S$	ΔU_{uv}	ΔU_{vv}
hexane (ttt)	18.037 ± 0.069	10.487 ± 0.310	7.550 ± 0.318	1.850 ± 0.048	8.636 ± 0.307
hexane (tgt)	17.811 ± 0.077	9.907 ± 0.362	7.904 ± 0.370	1.826 ± 0.054	8.081 ± 0.358
hexane (tgg)	16.970 ± 0.083	9.207 ± 0.402	7.763 ± 0.410	1.728 ± 0.058	7.479 ± 0.398
hexane (ggg)	15.317 ± 0.092	8.166 ± 0.453	7.151 ± 0.462	1.604 ± 0.065	6.562 ± 0.448

[a] Values reported in kcal/mol at 298 K.

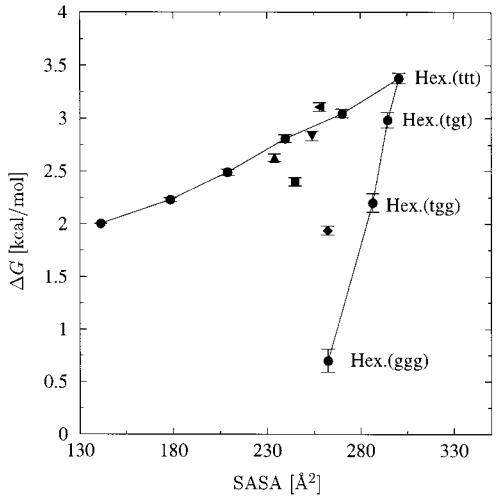

Figure 8. Calculated hydration free energies of the *n*-hexane rotamers (ttt, tgt, tgg, and ggg) compared with the alkane hydration free energies from Figure 3. Calculated free energies are shown taking as a reference the experimental hydration free energy of methane. See Figure 3 for the symbol keys.

hydrogens from hexane (ggg) all of the previously calculated hydration thermodynamic properties of cyclohexane were reproduced within statistical uncertainties.

The hydration free energies of the hexane rotamers are linearly related to the SASA. However, the linear scaling parameter γ of the hydration free energy of the hexane rotamers with respect to the SASA is very different from the scaling parameter corresponding to the alkane series from methane to hexane (ttt). A linear fit shows that for the normal alkane series from methane to hexane (ttt) $\gamma \simeq 9$ cal/(mol Å^2), while for the hexane rotamers we obtain $\gamma \simeq 70$ cal/(mol Å^2), a value almost 1 order of magnitude greater. Interestingly, the value of γ corresponding to the alkane cavities studied in this work ($\gamma \simeq 73$ cal/(mol Å^2)) is very similar to the one corresponding to the hexane rotamers.

These observations suggest that the variation in hydration free energies with conformational changes are dominated by the work of cavity formation. This is confirmed by examining the hydration thermodynamics of the hexane rotamer cavities (Table 6). The rotamer cavity hydration free energies scale linearly with the SASA; a linear scaling parameter of $\gamma \simeq 74$ cal/(mol Å^2) is obtained. Consequently, the cavity and total free energy changes in going from the ttt rotamer to the ggg rotamer are very similar, approximately −2.7 kcal/mol in either case. The entropic and enthalpic signatures are also very similar in the two cases. The ttt to ggg transition is favored equally by entropy and enthalpy for either the full or cavity rotamers.

The thermodynamics of the hexane rotamers can be rationalized by observing (see Table 5) that, even though there is a substantial SASA change, the solute−solvent interaction of hexane hardly changes in going from the ttt rotamer to the ggg rotamer. In these conformational transformations the solute−solvent interaction is almost totally uncorrelated with the SASA.

The good correlation between atomic composition and solute−solvent interaction energy and the corresponding poor correlation between the SASA and the solute−solvent interaction energy appears to be a general feature of hydrophobic hydration. Ashbaugh et al.[34] studied the conformational dependence of the hydration free energies of the linear alkanes. They observed that the hydration free energies of each alkane in different conformations correlate very well with the molecular surface area and that, moreover, the proportionality constant is similar for all of the alkanes and roughly equal to the proportionality constant measured for the corresponding alkane cavities. The observations of Ashbaugh et al. imply that the solute−solvent attractive interaction energy is only weakly dependent on molecular surface area and that, instead, it mainly depends on the atomic composition. A weak correlation between SASA and solute−solvent interaction energy was also observed by Pitarch et al.,[91] who observed that the interaction energy between the methane dimer and water is nearly independent of the methane−methane separation distance; they concluded that the cavity contribution is the main driving force for the hydrophobic interaction between the methane molecules.

3.5. Theoretical Estimates of the Work of Cavity Formation. In this paper the work of cavity formation of the alkanes in water is calculated by the FEP method. The method, although accurate, is computationally very intensive. It is therefore interesting from both a theoretical and practical point of view to compare the free energies of cavity formation calculated here with estimates from theoretical models such as scaled particle theory (SPT)[45] and information theory (IT).[46]

The reversible work associated with creating a void volume of a particular shape in a solvent is related to the probability p_0 of finding a natural occurrence of such a cavity in a sample of the pure solvent.[44] Both SPT and IT give estimates of p_0 and thus, ultimately, of the free energy of solvation of the cavity.

The SPT estimate of the free energy of hydration of the linear alkanes from 1 to 10 carbon atoms have been reported by Irisa et al.[92] They set to 1.99 Å the radius of all the CH_n groups ($n = 2$, 3, or 4) which are considered spherical. The excluded volume of water is also considered spherical with radius 1.375

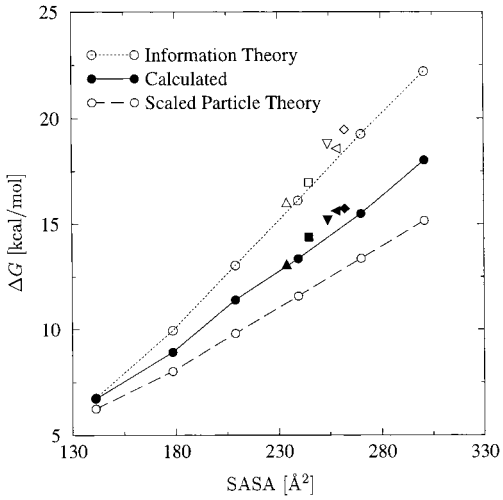

Figure 9. Comparison between calculation results and theoretical estimates of the free energies of alkane cavity formation in water.

Å. They employed the experimental values of the density of pure water at standard conditions.

To the best of our knowledge IT estimates of the work of cavity formation in water of a series of alkanes have not been previously reported. In the information theory approach, the probability of having zero water density in a specified region is estimated by extrapolating to zero, using the maximum entropy method, the probability distribution p_n of having n water molecules in the region.[54] Briefly, p_n is expressed as

$$p_n = \exp(\lambda_0 + \lambda_1 n + \lambda_2 n^2) \tag{19}$$

where the parameters (Lagrange multipliers) λ_i are set by the following conditions:

$$\sum_n p_n = 1 \tag{20}$$

$$\sum_n n_p n = \langle n \rangle \tag{21}$$

$$\sum_n n^2 p_n = \langle n^2 \rangle \tag{22}$$

Here $\langle n \rangle$ and $\langle n^2 \rangle$ are the averages of respectively the number of solvent molecules in the volume and the square of the number of solvent molecules in the volume. The value of p_0 is obtained by evaluating eq 19 at $n = 0$.

If ρ is the oxygen number density and $g(r)$ the oxygen−oxygen radial distribution function of water at the given thermodynamic conditions and v the volume of the cavity, $\langle n \rangle$ and $\langle n^2 \rangle$ are given by the relations

$$\langle n \rangle = \rho v \tag{23}$$

$$\langle n^2 \rangle - \langle n \rangle = \rho^2 \int_v \int_v \mathrm{d}\mathbf{r}\, \mathrm{d}\mathbf{r}'\, g(|\mathbf{r} - \mathbf{r}'|) \tag{24}$$

We have evaluated $g(r)$ from a simulation of TIP4P water at 298 K at atmospheric pressure; the volume v of each alkane cavity was obtained from the volume enclosed by the solvent accessible surface area of the cavity defined as specified in section 2.5. Equation 24 was evaluated by a Monte Carlo algorithm.[54]

The calculated free energies of hydration from Table 3 and the corresponding to theoretical estimates from SPT and IT are showed in Figure 9. The SPT estimate for the linear alkanes falls below the calculated values while the IT estimates fall above the calculated values. Both the SPT and IT results agree qualitatively with the calculated cavity free energies. They all predict a linear correlation between cavity hydration free energies and accessible surface area. The IT estimates reproduce quite accurately the ranking of the cavity free energies of the branched and cyclic alkanes with respect to the linear alkanes observed in the calculated free energies.

The origin of the deviations between the SPT cavity free energies and the calculations is difficult to assess, due to the fact that in the SPT work a quite different definition of the alkanes cavities was used than the one adopted here.

The deviation between the IT estimates and the calculations grows with alkane size. This deviation is not due to the definition of the hard cavities used in the IT estimates. The IT results can be brought into agreement with the FEP calculation only by reducing the carbon−water and hydrogen-water distances of closest approach to respectively 2.8 and 2.3 Å that correspond to a LJ repulsion for the soft cavities significantly larger than kT (about $3.4kT$). A measure of the effect of the softness of the repulsive potential used in the FEP calculations is the ratio between the calculated cavity−solvent average potential energy and the cavity hydration free energy $\Delta U_{uv}/\Delta G$; this ratio is zero for a hard cavity. From Table 3 we see that $\Delta U_{uv}/\Delta G$ is only of the order of 10%−15%. Moreover, we observed that the sensitivity of the information theory estimates to the cavity radii, of the values for $\langle n \rangle$ and $\langle n^2 \rangle$, and to the solvent density grows dramatically with cavity size. For instance, a 1% decrease in the values of $\langle n \rangle$ and $\langle n^2 \rangle$ produces a 10% decrease in the IT estimates of the cavity free energy of methane and a 50% decrease in the free energy of cavity formation of hexane. Because in IT the extent of the maximum entropy extrapolation grows with cavity size, the accuracy of the method decreases with increasing cavity size.

The hydration free energies are obtained by adding to the cavity hydration free energies the dispersion free energies. As was pointed out in section 3.3, in the case of the alkanes, these two terms are of nearly equal magnitude and opposite sign. Consequently, it is necessary to estimate each term very accurately in order to reproduce with reasonable accuracy the alkane hydration free energies. The IT estimates obtained here, although in qualitative agreement with the explicit solvent calculations, lack sufficient quantitative accuracy for this purpose.

3.6. Implications for Theories of Hydrophobicity. In this section we address the following questions: how does the thermodynamics of hydration of nonpolar compounds differ from that of polar compounds, and second, how does water differ from other liquids as a solvent for nonpolar solutes? This issue is analyzed both from the perspective of the numerical results we have obtained as well as experimental data.

Entropy loss dominating the free energy change is the signature of hydrophobic hydration.[48] In the iceberg model of hydrophobicity,[11] the entropy loss upon dissolution of apolar gases in water was explained in terms of an enhanced local structuring of water near the solute. However, other studies[19,20] concluded that the unusually large entropy loss can be explained in terms of the small size of the water molecules and it is not necessary to invoke, as in the iceberg model, a loss of orientational entropy of the water molecules near the solute.

Rather than focus on entropy as the "hydrophobic signature", we suggest that hydrophobic molecules are distinguished from hydrophilic ones by their much smaller enthalpy gain upon dissolution in water. The fact that polar species exhibit similar

entropies of hydration as nonpolar species of similar size and shape supports this view.[93] In this view polar molecules are more soluble in water because they can form very favorable electrostatic interactions with water and not because they induce a small entropy loss. For example, the free energy of inserting a water molecule in water at standard conditions is approximately −6 kcal/mol [60] to be compared with the free energy of hydration of methane that is approximately 2 kcal/mol.[60] This difference is mostly due the difference of hydration enthalpies (about −10 kcal/mol for water and about −2.5 kcal/mol for methane[60]), whereas the differences in hydration entropies are quite small (at room temperature for water $-T\Delta S \simeq 3.6$ kcal/mol and for methane $-T\Delta S \simeq 4.7$ kcal/mol [60]). The entropy loss can be viewed as being in part caused by the loss of orientational freedom of the water molecules near the solute that have fewer opportunities to form stable hydrogen bonds with other water molecules. The solvent excluded volume created by the solute is also responsible for entropy loss due to the reduced number of solvent configurations in the solution in which solute−solvent overlaps are avoided. The latter is referred to as translational entropy loss and the former as orientational entropy loss.[94] Madan and Lee[19] and Durell and Wallqvist[20] have both considered this question. They concluded that the small size of the water molecules rather than the hydrogen bond structure of water characterize hydrophobic effects. Durell & Wallqvist,[20] in addition, compared the entropy loss for insertion of a nonpolar solute in water with the corresponding value for insertion of a nonpolar solute in a nonpolar liquid with molecular volume and density the same as those of water. They observed small differences between the two solvation entropies. Given that the orientational freedom of a water molecule near a hydrophobic solute should be strongly dependent on directional hydrogen-bonding interactions and that such interactions are absent in a nonpolar solvent, this indicates that the loss of orientational freedom of the water molecules near the solute is not a major cause of the hydration entropy loss. This view is further supported by the observation that the experimental hydration entropies are generally only weakly correlated with the polarity of the solute. If the orientational entropy loss were a major component of the thermodynamics of hydrophobic hydration, a stronger dependence of the hydration entropy on solute polarity would be expected. Consequently, the loss of orientational entropy of the water molecules in contact with the solute appears to have only a secondary role in hydration thermodynamics of small apolar solutes. These observations are in conflict with the iceberg model of hydrophobic hydration.

Finally, we comment on the ability of water to reorganize around a cavity. The water reorganization energy upon cavity formation is determined by two factors: (i) the loss of hydrogen bonding partners for the water molecules in contact with the cavity; (ii) the reorganization of the water network around the cavity. To understand the role of the two factors consider the hypothetical process whereby a void the size of a water molecule is created in a pure water sample in which the solvent around the cavity is not allowed to reorganize. Only the water bulk far from the cavity reorganizes by accepting the water molecule displaced by the cavity. The process (see Figure 10) is thermodynamically equivalent to a two-step process in which a tagged water molecule is extracted from a rigid water lattice and subsequently inserted in a liquid water sample. Given that the solvent−cavity interaction energy is zero, the solvent reorganization energy for this process is equal to the total average potential energy change $\Delta\bar{U}$. In the first step the potential energy change is $-B$, where B is the water binding

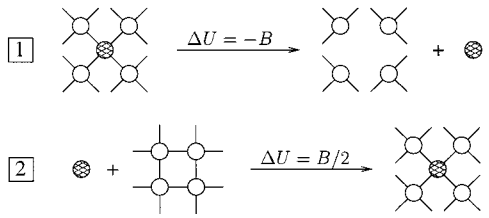

Figure 10. Creation of a void the size of a water molecule in water without solvent reorganization. Process 1 is the extraction of a tagged water molecule from the rigid water lattice; process 2 is the introduction of the tagged water molecule in the water bulk.

energy. In the second step the system regains half of the energy lost in the first step. It follows that the solvent reorganization energy for this hypothetical process is predicted to be $-B/2$ or about 10 kcal/mol.

The calculated values of the solvent reorganization energy upon methylation of an alkane cavity chain (Table 2), ranging from 1 to 2 kcal/mol, are much less than what is predicted by the rigid water solvation model above. The difference is due to the rearrangement of the hydration shell around the cavity. The water molecules are therefore able to reorient themselves to form a structure around the cavity that minimizes the loss of hydrogen-bonding contacts and/or reinforces existing contacts. Thus, the plasticity of the hydrogen-bonding network of water at standard conditions is such that a small energy penalty is paid to form voids about the size of a water molecule. The thermodynamic characteristics of hydrophobic hydration at room temperature can be therefore ascribed to the ability of water to efficiently reorganize around an impenetrable volume better than other solvents.[12] At room temperature the voids are hydrated by low-energy water structures that are believed to disappear at higher temperatures in correspondence with a lowering of the solubilities of simple hydrophobic species.[95] At even higher temperatures, as in non hydrogen-bonded liquids, the solubilities increase due to large energy fluctuations that induce the formation of transient cavities.[17]

4. Conclusions

This study reports the first complete description of the solution thermodynamics of alkanes in water by computer simulations, including the enthalpy and entropy changes in addition to the solvation free energies. We have also obtained a complete thermodynamic description of the solvation of the associated alkane cavities.

The molecular force field (OPLS-AA)[68] used in this study is found to generally reproduce the experimental free energies, enthalpies, and entropies of hydration of the hydrocarbons examined. In a previously reported study on methyl-substituted amines with a different force field,[96] discrepancies between calculated and experimental hydration free energies were shown to be due to much larger, qualitative discrepancies between the experimental and simulation results for enthalpies and entropies. [Much better agreement is obtained with recently published[97] OPLS parameters for these compounds.[87]] The fact that, for the alkanes, not only the hydration free energies but also the calculated hydration entropies and enthalpies are in agreement with the experiments is an indication that the model is able to capture the essential physics of alkane hydration.

Although difficult to calculate[17,18,20] and unnecessary for the calculation of hydration free energies,[80] the solvent reorganization energy is found to be a large component of the total enthalpy of hydration. We find that solvent reorganization alone[77,78] does not account for the observed entropy-enthalpy compensation effects.

The larger solubility of the cyclic alkanes with respect to the linear alkanes is due to their more favorable solute−solvent interaction energies per unit surface area. This phenomenon is explained by the finding that the solute−solvent interaction energies are almost independent of the SASA. Evidently, due to steric effects and specific water−water interactions, "saturation" occurs, whereby increasing the solvent accessible area of the solute does not necessarily cause a proportional increase in the solute−solvent van der Waals contacts for molecules of this size.

The thermodynamics of hydrophobic hydration has been interpreted in the past in terms of two competing models: (a) local structuring of the water solvent;[11,17] or (b) large entropy loss due to the small size of the water molecules, which decreases the probability of finding larger solvent cavities.[19,20] The findings of this work support the latter model more than the former. By observing that the hydration entropies of hydrophobic compounds are similar in magnitude to the hydration entropies of polar compounds of similar size and shape, we suggest that the hydration entropies are determined mainly by the loss of translational entropy caused by the inhomogeneity introduced into the system by the presence of the solute and only secondarily by the orientational entropy loss of the water molecules in the hydration shell. Moreover, it is not necessary to invoke local water structuring to explain the observed favorable hydration enthalpies. We find that the favorable hydration enthalpies of the alkanes are caused by the large and attractive solute−solvent dispersion interactions and by the surprisingly small water reorganization energies. The water-hydrogen bonding network is interpreted as being extremely plastic and able to adapt to the shape of the solute with minor energetic and entropic losses. These effects, which are specific to water, offer an explanation of the finding that at room temperature water hydrates small hydrophobic solutes as well, if not better, than nonpolar solvents of similar molecular size and density.[17,19,20]

By decomposing the hydration process into cavity formation plus solute insertion in the cavity, we observe that hydration entropies and solvent reorganization energies are largely determined by cavity formation whereas solute insertion modifies only the solute−solvent interaction energies. The work of cavity formation is not mostly entropic as a hard sphere model would suggest. Instead, the process leads to a substantial solvent reorganization energy but much less unfavorable than what would be expected if the solvent was not allowed to reorganize. The hydrophobic hydration theories examined (information theory and scaled particle theory) that focus only on the work of cavity formation, although in qualitative accord with our results, are found to lack sufficient accuracy to quantitatively predict alkane hydration free energies.

The findings presented in this paper suggest that an empirical parametrization of the hydration free energy and the free energy of association of apolar species based only on the solvent accessible surface area is insufficient. Successful parametrization should contain a surface area term to reproduce effects due to entropy loss and solvent reorganization energy and terms that depend on the number, location, and type of atomic interaction centers to reproduce effects due to the solute−solvent dispersion interactions which are only weakly correlated with surface area.

Acknowledgment. This work has been supported in part by NIH Grants GM-30580 and RR-06892. We thank Dr. Anders Wallqvist and Dr. Nobuyuki Matubayasi for many discussions and for sharing their insights about hydrophobic hydration.

References and Notes

(1) Franks, F., Ed. *Water, A Comprehensive Treatise*; Plenum: New York, 1972−1982; Vols. 1−7.
(2) Ben-naim, A. *Hydrophobic Interactions*; Plenum Press: New York, 1980.
(3) Tanford, C. *The hydrophobic effect: formation of micelles and biological membranes*; Wiley: New York, 1973.
(4) Dill, K. *Biochemistry* **1990**, *29*, 7133−7155.
(5) Privalov, P.; Makhatadze, G. *J. Mol. Biol.* **1993**, *232*, 660−679.
(6) Honig, B.; Yang, A. *Adv. Protein Chem.* **1995**, *46*, 27−58.
(7) Sturtevant, J. *Proc. Natl. Acad. Sci. U.S.A.* **1977**, *74*, 2236−2240.
(8) Williams, D.; Searle, M.; Mackay, J.; Gerhard, U.; Maplestone, R. *Proc. Natl. Acad. Sci. U.S.A.* **1993**, *90*, 1172−78.
(9) Froloff, N.; Windemuth, A.; Honig, B. *Protein Sci.* **1997**, *6*, 1293−1301.
(10) *Faraday Discuss.* **1996**, 103.
(11) Frank, H.; Evans, M. *J. Chem. Phys.* **1945**, *13*, 507−532.
(12) Lee, B. *Biopolymers* **1985**, *24*, 813−23.
(13) Levy, R.; Gallicchio, E. *Annu. Rev. Phys. Chem.* **1998**, *49*, 531−67.
(14) Straatsma, T.; Berendsen, J.; Postma, J. *J. Chem. Phys.* **1986**, *85*, 6720.
(15) Zichi, D.; Rossky, P. *J. Chem. Phys.* **1986**, *84*, 2814−2822.
(16) Jorgensen, W.; Blake, J.; Buckner, J. *Chem. Phys.* **1989**, *129*, 193.
(17) Guillot, B.; Guissani, Y. *J. Chem. Phys.* **1993**, *99*, 8075.
(18) Matubayasi, N.; Reed, L.; Levy, R. *J. Phys. Chem.* **1994**, *98*, 10640.
(19) Madan, B.; Lee, B. *Biophys. Chem.* **1994**, *51*, 279−289.
(20) Durell, S.; Wallqvist, A. *Biophys. J.* **1996**, *71*, 1695.
(21) Pangali, C.; Rao, M.; Berne, B. J. *J. Chem. Phys.* **1979**, *71*, 2975−2981.
(22) Watanabe, K.; Anderesen, H. *J. Phys. Chem.* **1986**, *90*, 795−802.
(23) Smith, D.; Haymet, A. *J. Chem. Phys.* **1993**, *98*, 6445.
(24) New, M.; Berne, B. *J. Am. Chem. Soc.* **1995**, *117*, 7172−7179.
(25) Wallqvist, A.; Berne, B. J. *J. Phys. Chem.* **1994**, *99*, 2885−2892.
(26) Honig, B.; Sharp, K.; Yang, A. *J. Phys. Chem.* **1993**, *97*, 1101−9.
(27) Lazaridis, T.; Archontis, G.; Karplus, M. *Adv. Protein Chem.* **1995**, *47*, 262−344.
(28) Simonson, T. *Int. J. Quantum Chem.* **1999**, *73*, 45−57.
(29) Roux, B.; Simonson, T. *Biophys. Chem.* **1999**, *78*, 1.
(30) Ooi, T.; Oobatake, M.; Nemethy, G.; Sheraga, A. *Proc. Natl. Acad. Sci. U.S.A.* **1987**, *84*, 3086.
(31) Sitkoff, D.; Sharp, K.; Honig, B. *Biophys. Chem.* **1994**, *51*, 397−409.
(32) Wallqvist, A.; Covell, D. *J. Phys. Chem.* **1995**, *99*, 13118−13125.
(33) Ashbaugh, H.; Kaler, E.; Paulaitis, M. *Biophys. J.* **1998**, *75*, 755−768.
(34) Ashbaugh, H.; Kaler, E.; Paulaitis, M. *J. Am. Chem. Soc.* **1999**, *121*, 9243−9244.
(35) Jorgensen, W.; Gao, J.; Ravimohan, C. *J. Phys. Chem.* **1985**, *89*, 3470.
(36) Wallqvist, A. *J. Phys. Chem.* **1991**, *95*, 8921−27.
(37) Wallqvist, A.; Covell, D. *Biophys. J.* **1996**, *71*, 600−608.
(38) Mountain, R.; Thirumalai, D. *Proc. Natl. Acad. Sci. U.S.A.* **1998**, *95*, 8436−40.
(39) Sun, Y.; Spellmeyer, D.; Pearlman, D.; Kollman, P. *J. Am. Chem. Soc.* **1992**, *114*, 6798.
(40) Kaminski, G.; Duffy, E.; Matsui, T.; Jorgensen, W. *J. Phys. Chem.* **1994**, *98*, 13077−13082.
(41) Radmer, R.; Kollman, P. *J. Comput. Chem.* **1997**, *18*, 902−19.
(42) Pratt, L.; Chandler, D. *J. Chem. Phys.* **1977**, *67*, 3683−3704.
(43) Pratt, L.; Chandler, D. *J. Chem. Phys.* **1980**, *73*, 3434−41.
(44) Widom, B. *Chem. Phys.* **1982**, *86*, 869.
(45) Pierotti, R. *Chem. Rev.* **1976**, *76*, 717−26.
(46) Hummer, G.; Garde, S.; García, A.; Pohorille, A.; Pratt, L. *Proc. Natl. Acad. Sci. U.S.A.* **1996**, *93*, 8951−8955.
(47) Gallicchio, E.; Kubo, M.; Levy, R. *J. Am. Chem. Soc.* **1998**, *120*, 4526−27.
(48) Ben Naim, A. *Water and Aqueous Solutions*; Plenum: New York, 1974.
(49) Guillot, B.; Guissani, Y.; Bratos, S. *J. Chem. Phys.* **1991**, *95*, 3643.
(50) Lazaridis, T.; Paulaitis, M. *J. Phys. Chem.* **1994**, *98*, 635−642.
(51) Lee, B. *Biopolymers* **1991**, *31*, 993−1008.
(52) Lazaridis, T.; Paulaitis, M. *J. Phys. Chem.* **1992**, *96*, 3847−3855.
(53) Ben-Naim, A. *J. Phys. Chem.* **1978**, *82*, 874−85.
(54) Hummer, G.; Garde, S.; García, A.; Paulaitis, M.; Pratt, L. *Phys. Chem. B* **1998**, *102*, 10469−82.
(55) Beveridge, D.; Di Capua, F. *Annu. Rev. Biophys. Chem.* **1989**, *18*, 431.
(56) Jorgensen, W. *Acc. Chem. Res.* **1989**, *22*, 184.
(57) Warshel, A.; Sussman, F.; King, G. *Biochemistry* **1986**, *25*, 8368.
(58) Kollman, P. *Chem. Rev.* **1993**, *93*, 2395.

(59) Wallqvist, A.; Berne, B. *J. Phys. Chem*. **1995**, *99*, 2893−2899.
(60) Ben-Naim, A.; Marcus, Y. *J. Chem. Phys*. **1984**, *81*, 2016.
(61) Qian, H.; Hopfield, J. *J. Chem. Phys*. **1996**, *105*, 9292.
(62) Jorgensen, W.; Chandrasekhar, J.; Madura, J. *J. Chem. Phys*. **1983**, *79*, 926−935.
(63) Matubayasi, N.; Levy, R. *J. Phys. Chem*. **1996**, *100*, 2681.
(64) Matubayasi, N.; Gallicchio, E.; Levy, R. *J. Chem. Phys*. **1998**, *109*, 4864−72.
(65) Nemethy, G.; Sheraga, H. *J. Chem. Phys*. **1962**, *36*, 3401.
(66) Lazaridis, T. *J. Phys. Chem. B* **1998**, *102*, 3531−41.
(67) Jorgensen, W.; Chandrasekhar, J.; Madura, J.; Impey, R.; Klein, M. *J. Chem. Phys*. **1983**, *79*, 926.
(68) Jorgensen, W.; Maxwell, D.; Tirado-Rives, J. *J. Am. Chem. Soc*. **1996**, *118*, 11225.
(69) Kaminski, G.; Duffy, E.; Matsui, T.; Jorgensen, W. *J. Phys. Chem*. **1994**, *98*, 13077.
(70) Allen, M.; Tildesley, D. *Computer Simulation of Liquids*; Oxford University Press: New York, 1993.
(71) Weeks, J.; Chandler, D.; Andersen, H. *J. Chem. Phys*. **1971**, *54*, 5237−47.
(72) Beglov, D.; Roux, B. *J. Chem. Phys*. **1994**, *100*, 9050−9062.
(73) Connolly, M. *J. Appl. Crystallogr*. **1983**, *16*, 548−558.
(74) Connolly, M. *J. Am. Chem. Soc*. **1985**, *107*, 1118−24.
(75) Blokzijl, W.; Engberts, J. *Angew. Chem., Int. Ed. Engl*. **1993**, *32*, 1545−1579.
(76) Kaminski, G.; Jorgensen, W. Personal communication.
(77) Ben-Naim, A. *Biopolymers* **1975**, *14*, 1337−1355.
(78) Grunwald, E.; Steel, C. *J. Am. Chem. Soc*. **1995**, *117*, 5687−5692.
(79) Lumry, R.; Rajender, S. *Biopolymers* **1970**, *9*, 1125−1227.
(80) Yu, H.; Karplus, M. *J. Chem. Phys*. **1988**, *89*, 2366.
(81) Prévost, M.; Oliveira, I.; Kocher, J.; Wodak, S. *J. Phys. Chem*. **1996**, *100*, 2738−43.
(82) Postma, J.; Berendsen, H.; Haak, J. *Faraday Symp. Chem. Soc*. **1982**, *17*, 55.
(83) Lee, B. J. *Chem. Phys*. **1985**, *83*, 2421−25.
(84) Beutler, T.; Béguelin; van Gunsteren, W. *J. Chem. Phys*. **1995**, *102*, 3787.
(85) Pohorille, A.; Pratt, L. *J. Am. Chem. Soc*. **1990**, *112*, 5066−74.
(86) Berne, B. *Proc. Natl. Acad. Sci. U.S.A*. **1996**, *93*, 8800−8803.
(87) Kubo, M.; Gallicchio, E.; Levy, R. Manuscript in preparation.
(88) Carlson, H.; Jorgensen, W. *J. Phys. Chem*. **1995**, *99*, 10667−73.
(89) Hawkins, G.; Cramer, C.; Truhlar, D. *J. Phys. Chem. B* **1997**, *101*, 7147−57.
(90) Sitkoff, D.; Ben-Tai, N.; Honig, B. *J. Phys. Chem*. **1996**, *100*, 2744−52.
(91) Pitarch, J.; Moliner, V.; Pascual-Ahuir, J.; Silla, A.; Tuñón, I. *J. Phys. Chem*. **1996**, *100*, 9955−9959.
(92) Irisa, M.; Nagayama, K.; Hirata, F. *Chem. Phys. Lett*. **1993**, *207*, 430−5.
(93) Cabani, S.; Gianni, P.; Mollica, V.; Lepori, L. *J. Solution. Chem*. **1981**, *10*, 563.
(94) Ashbaugh, H.; Paulaitis, M. *J. Phys. Chem*. **1996**, *100*, 1900−1913.
(95) Fernandez-Prini, R.; Crovetto, R. *J. Phys. Chem. Ref. Data* **1989**, *18*, 1231.
(96) Kubo, M.; Gallicchio, E.; Levy, R. *J. Phys. Chem*. **1997**, *101*, 10527−10534.
(97) Rizzo, R.; Jorgensen, W. *J. Am. Chem. Soc*. **1999**, *121*, 4827−4836.